

Designing an optimal ion adsorber at the nanoscale: the unusual nucleation of AgNPs/Co²⁺-Ni²⁺ binary mixtures

Pietro Corsi,[†] Iole Venditti,[†] Chiara Battocchio,[†] Carlo Meneghini,[†] Fabio Bruni,[†] Paolo Proposito,[‡] Federico Mochi,[‡] and Barbara Capone^{*,†}

[†]*Dipartimento di Scienze, Università degli Studi Roma Tre, Via della Vasca Navale 84, 00146, Roma, Italy*

[‡]*Dipartimento di Ingegneria Industriale, Università degli Studi di Roma Tor Vergata, Via del Politecnico, 1, 00133 Roma, Italy*

E-mail: barbara.capone@uniroma3.it

Abstract

Selective removal of heavy metals from water is a complex topic. We present a theoretical-computational approach, supported by experimental evidences, to design a functionalised nanomaterial able to selectively capture metallic ions from water within a self-assembling process. A theoretical model is used to map an experimental mixture of Ag nanoparticles (AgNPs) and either Co²⁺ or Ni²⁺ onto an additive highly asymmetric attractive Lennard-Jones binary mixture. Extensive NVT (constant number of particles, volume and temperature) Monte Carlo simulations are performed to desume the set of parameters that first induce aggregation amongst the two species in solution, and then affect the morphology of the aggregates. The computational predictions are thus compared to the experimental re-

sults. The gathered insights can be used as guidelines for the prediction of an optimal design of a new generation of selective nanoparticles to be used for metallic ion adsorption hence for maximising the trapping of ions in an aqueous solution.

Keywords *Nanoparticles, Ion Adsorption, Driven Self-Assembly, Transition Metal, Metallic Ions, Monte Carlo Simulations, Theoretical Predictions*

Introduction

The ability to isolate and recognise heavy metal ions in water is becoming a very active field of study and research due to the impact the heavy metals have on the environment and health.¹⁻⁴ To tackle this issue nanotechnologies are starting to play a key role in designing and developing tunable systems able to selectively sense the presence of such pollutants.⁵⁻¹⁸

Silver nanoparticles (AgNPs) coated with thiols have been proven to be a very effective tool for detection and removal of heavy metals in aqueous solutions.¹⁹⁻²¹ Their ability to selectively interact and induce nucleation of the latter, has been recently shown^{22,23} in the case in which colloidal AgNPs, functionalised with 3-mercapto-1-propanesulfonic acid sodium salt (3-MPS), are dispersed in aqueous solutions containing either Co^{2+} or Ni^{2+} ions. In particular, the well dispersed AgNPs, tend to aggregate when Co^{2+} or Ni^{2+} ions are present in solution giving rise to a complex clustering process. The average diameter of the nanoparticles has been measured by means of a Dynamic Light Scattering characterisation, and a TEM analysis of the AgNPs, both in presence and in absence of the metallic ions. AgNPs without contaminant have a diameter of 8.5 nm. Conversely, the average size measured in solutions of AgNPs and either Co^{2+} or Ni^{2+} is of several tens of nanometers, indicating that the nanoparticles undergo a clustering process upon adsorption of these ions.²² However, the self-assembly scenario of the binary mixtures is quite different for the two heavy metal ions: notwithstanding having almost the same ionic radius and same valence, Co^{2+} induces the

nucleation of almost packed micelles of AgNPs while in the exact same conditions (concentration, temperature, pH) Ni^{2+} induces the aggregation of branched structures as shown in Figure 1.²²

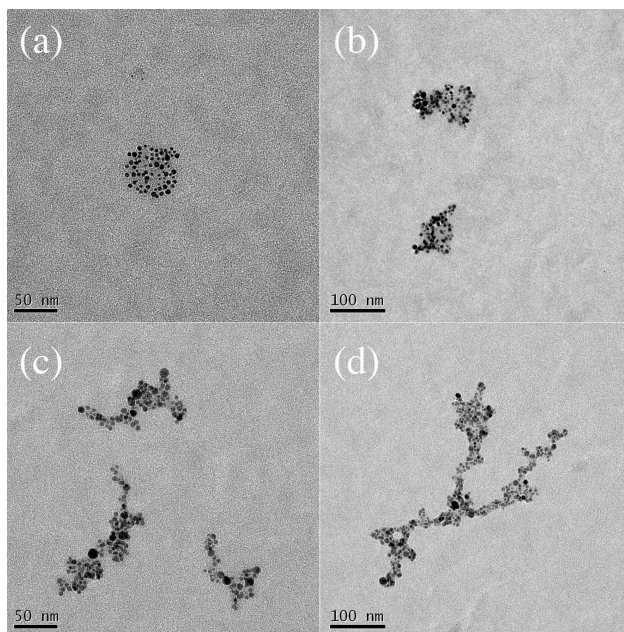


Figure 1: Self-assembled structures from TEM (Transmission Electron Microscope). Top panels show self-assembled structures of the AgNPs/ Co^{2+} nanocomposite where 1 ppm of Co^{2+} has been dispersed in solution. Bottom panels show self-assembled structures of the AgNPs/ Ni^{2+} nanocomposite at the same ion concentration.

It is noteworthy that all AgNPs, whose morphologies are reported in Figure 1, have a constant thiol grafting density. Such nanoparticles have been already object of several experimental characterisations used to assess the nanoparticles size, their monodispersity, and the consistency in the grafting density.²² Throughout this paper, the thiol coating of the nanoparticles used as a reference, remains constant for all considered nanoparticles and unchanged throughout all performed experiments. The theoretical predictions that will be presented in the following parts of this paper will serve to assess how the different and competing effects in the system (particle size, effective interaction between the diverse species) affect the self-assembling properties of the mixtures of AgNPs and heavy metals. Such an understanding promise to design, for different ions, nanoparticles with optimal adsorption properties.

In order to do this, we decided to perform an extensive computational analysis simplifying the system by coarse graining all of the details, while retaining a reduced set of informations relevant to reproduce the general characteristics leading to the peculiar self-assembling properties shown experimentally. To start with, both ions and colloids are represented as spherical particles interacting through an isotropic potential. Solvent-particles interaction are considered to be implicit: the solvent is replaced by an effective pairwise attraction between the two colloidal species. In particular we will make use of the implicit Lennard-Jones (LJ) model where the solvent is replaced by a pairwise additive LJ interaction between nanoparticles. A stronger interaction between the diverse nanoparticle species, corresponds to an increase in the well depth in the LJ interaction.

To mimic the effect of the intrinsic nature of each metallic ion (e.g. electronic structure, hydration properties) while interacting with the AgNPs in solution, we explored different size ratios and different interaction strengths between ions and nanoparticles on the self assembly scenario. Ions in solution do interact with the nanoparticles by means of an effective interaction that is screened by the presence of the solvent that, in the experimental case investigated, is water. Co^{2+} and Ni^{2+} are transition metal ions having almost identical ionic radius,²⁴ but different hydration radius.²⁵ In a simplified picture, the different hydration shells lead to a difference in both effective size and in the effective attraction strength that the ions feel when interacting with the coated AgNPs.

Methods

Aim of this work is to map the experimental systems considered in ref.²² into a theoretical model that allows to separately investigate the effects of a manifold of parameters on the aggregation process. We decided to map the complex experimental nanoparticles into a simplified description that allows to investigate separately the effect of the effective interaction, and the effect of a diverse size ratio between AgNPs and ions. For these reasons all systems

are represented as additive asymmetric LJ binary mixtures made of particles of diameter $\sigma_{(i,n)}$ (where i indicates the metallic ions, and n indicates the nanoparticles) interacting by means of a total potential made of a repulsive term v_0 and an attractive term $\lambda_{(i,n)}v_{\text{att}}(\mathbf{r})$ that will be used to tune the interaction between the ions i and the colloidal nanoparticles n .

$$v(\mathbf{r}, \lambda) = v_0(\mathbf{r}) + \lambda_{(i,n)}v_{\text{att}}(\mathbf{r}), \quad (1)$$

where:

$$v_0(\mathbf{r}) = \begin{cases} 4\epsilon \left[\left(\frac{\sigma_{(i,n)}}{r} \right)^{12} - \left(\frac{\sigma_{(i,n)}}{r} \right)^6 + \frac{1}{4} \right] & \text{for } r \leq 2^{1/6}\sigma_{(i,n)} \\ 0 & \text{for } r > 2^{1/6}\sigma_{(i,n)} \end{cases} \quad (2)$$

and

$$v_{\text{att}}(\mathbf{r}) = \begin{cases} -\epsilon & \text{for } r \leq 2^{1/6}\sigma_{(i,n)} \\ 4\epsilon \left[\left(\frac{\sigma_{(i,n)}}{r} \right)^{12} - \left(\frac{\sigma_{(i,n)}}{r} \right)^6 \right] & \text{for } r > 2^{1/6}\sigma_{(i,n)} \end{cases} \quad (3)$$

The attractive interaction between the two species, $\lambda_{(i,n)}$ is a symmetrical 2×2 matrix of the kind:

$$\lambda_{(i,n)} = \begin{pmatrix} \lambda_{j,j} & \lambda_{j,k} \\ \lambda_{k,j} & \lambda_{k,k} \end{pmatrix} \quad (4)$$

where $j, k \in (i, n)$. In the following, the interaction between identical species will be considered as repulsive $\lambda_{(i,i)} = \lambda_{(n,n)} = 0$, while the diagonal terms $\lambda_{(i,n)} = \lambda_{(n,i)}$ indicate the interaction between ions and nanoparticles.

The role of λ is to control the strength of the attraction between the nanoparticles; for $\lambda = 0$ we recover the full, generalised Lennard-Jones potential.²⁶ The main quantities that we will use to characterise the system are: the ratio $q = R_n/r_i$ between the radius $R_n = \sigma_n/2$ of the nanoparticles and that $r_i = \sigma_i/2$ of the ions; the *total* volume fraction of the system $\phi = \frac{4}{3}\pi(n_i r_i^3 + N_n R_n^3)/V$, e.g. the ratio between the volume occupied by both ions and nanoparticles and the total available volume, n_i and N_n being the total number of ions and

nanoparticles respectively. The third quantity that we will focus on, is the parameter that tunes the cross attractive interaction $\lambda_{(i,n)}$ between ions and nanoparticles. Finally we have analysed the effect due to an increase in the number n_i of ions for fixed $(q, \phi, \lambda_{(i,n)})$ on the self-assembling properties of the system.

Experimentally all of the ion-nanoparticle binary mixtures present a size ratio of the order of $q \sim 10$, the silver nanoparticles being of $R_n \sim 1.2$ nm while $r_{Ni^{2+} \sim Co^{2+}} \sim 0.1$ nm. Upon increasing density of ions in solution, the binary mixtures undergo a self-assembly path that produces very different aggregates for the two systems containing one or another metallic ion.²² As it is well known, the red shift and the broadening of the plasmonic bands in the UV visible spectra are indicative of both aggregation process and polydispersity of the metal nanoparticles.²⁷⁻²⁹ In this case, the shifts and the broadening of the plasmonic bands are a function of the percentage of ions in solution, allowing to extrapolate the dependence of the average growth rate of the aggregates on the chemical nature of the nanocomposites.³⁰ The mean size of the elongated clusters that spontaneously self-assemble in the $Ni^{2+}/AgNPs$ mixtures, grows with a much steeper slope with respect to the almost spherical-like aggregates self-assembled by the $Co^{2+}/AgNPs$ mixtures, see Figure 2. Such a phenomenon seems to indicate that non spherical aggregates are more keen to grow when the concentration of ions in solution is increased.

To assess what are the key parameters that influence the final outcome of the clustering process, e.g. cluster size and conformation, ion adsorption and distribution in the aggregates, density dependence of the whole clustering process, simulations in the NVT ensemble have been performed for systems with $N_n = 300$ nanoparticles, and $n_i = 600, 900, 1200$ and 1500 ions, focusing on the aggregation properties of binary mixtures for a fixed sets of values of ϕ , for two different values of $\lambda_{(i,n)} = (3, 5)$ and two very different values of the size ratio $q = (5, 10)$.

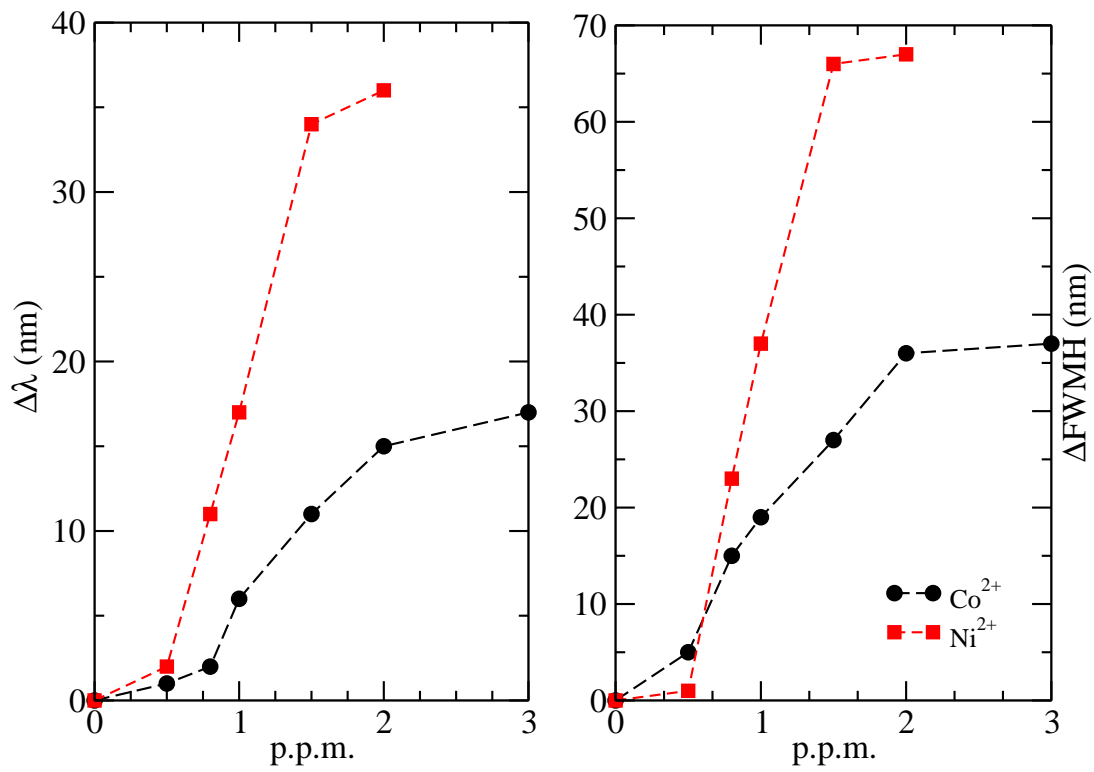


Figure 2: Shift $\Delta\lambda$, and broadening $\Delta FWHM$ of the plasmonic bands as a function of increasing density of ions for solutions of AgNPs nanoparticles in the presence of Co^{2+} (black circles) and Ni^{2+} (red squares). The dashed line is a guide to the eye.

Results

The analysis of the single cluster properties, namely the dependence of the mean aggregation number, distribution of ions and colloids within the aggregates, end shape on equilibration time, as a function of $(q, \phi, \lambda_{(i,n)}, n_i)$ highlights how the choice of the different parameters drives the self-assembly process in the phase space. All system studied self-assemble into aggregates made of a mixture of ions and nanoparticles.

The average number of colloids belonging to each cluster (mean aggregation number) is shown in Figure 3 for the four (q, λ) combinations, four different values of the number of ions per fixed volume fraction, and for a set of five distinct volume fractions $\phi \in [0.01, 0.1]$. In all of the four panels n_i increases along the x -axis as a multiple of the number of nanoparticles, and ϕ grows along the y axis.

The parameter q clearly influences the mean aggregation number for both species, as shown in Figure 3 panels (a)-(b) for $q = 5$ and $\lambda = 3$ and 5 respectively, and (c)-(d) for $q = 10$ and $\lambda = 3$ and 5 . For fixed ionic size, smaller nanoparticles ($q = 5$) are lead to the formation of clusters with a higher mean aggregation number as compared to bigger nanoparticles ($q = 10$). Moreover clusters assembled for $q = 5$ adsorb more ions per cluster than the ones with $q = 10$ (resulting in a higher mean aggregation number of ions per cluster, not shown here).

A change in λ has an evident effect on the internal structure of the clusters as well as on the equilibration of the latter. A stronger attraction ($\lambda = 5$) favours the clustering of the nanoparticles, and ions form quite “rapidly” (fewer of MC steps) a well defined core within the clusters leading to a lower mean aggregation number (there are no exposed ions that let the aggregation process to continue). Conversely a weaker cross-interaction ($\lambda = 3$) is not able to induce a complete segregation, leaving clustered ions exposed to the solvent thus favouring the aggregation of more and more nanoparticles.

To better understand the inner structure of the clusters, we quantify the segregation of the ions within the clusters. We thus introduce the parameter s as the average distance

between the centre of mass of the ions and that of the nanoparticles, renormalised by the average size of the clusters:

$$s = \frac{\sum_{r_n} r_n P(r_n) - \sum_{r_i} r_i P(r_i)}{\sum_{R_g} R_g P(R_g)}, \quad (5)$$

where $P(x)$ is the normalised probability density distribution of x averaged over equilibrium configurations, and $R_g^c = \sqrt{\frac{1}{N_n^c} \sum_{i=1}^{N_n^c} (r_i^c - r_{cm}^c)^2}$ is the nanoparticles radius of gyration of the c -th cluster estimated as the average distance of the nanoparticles from the centre of mass.

The $s \gg 0$ limit indicates an inclusion of the ions in an aggregate whose outer shell is made of nanoparticles. A negative value of s would mean a strong exposure of the ions. $s \simeq 0$ is for systems that have an even distribution of ions and nanoparticles in the aggregates.

Weak λ interactions lead to an almost even distribution of ions in the clusters (lower values of s), thus leaving ions exposed to the solvent- see panels (a), (c) and (e) of Figure 4. In such a case clusters can keep growing till the excluded volume of the nanoparticles arrests the aggregation process.

On the other hand, the stronger the cross-interaction, the more ions and nanoparticles are segregated - see panels (d) and (f) of Figure 4. A bigger λ leads to a higher value of s favouring the complete adsorption of the ions in the aggregates - panel (b). The steric repulsion between the bigger nanoparticles will then arrest more rapidly the aggregation process.

The present computational analysis aims at highlighting how to design the optimal nanoparticles able to selectively capture and retain ions in solution; optimal ion removal systems are those able to separate ions from the capturing agents (nanoparticles) while insulating them from the solution.

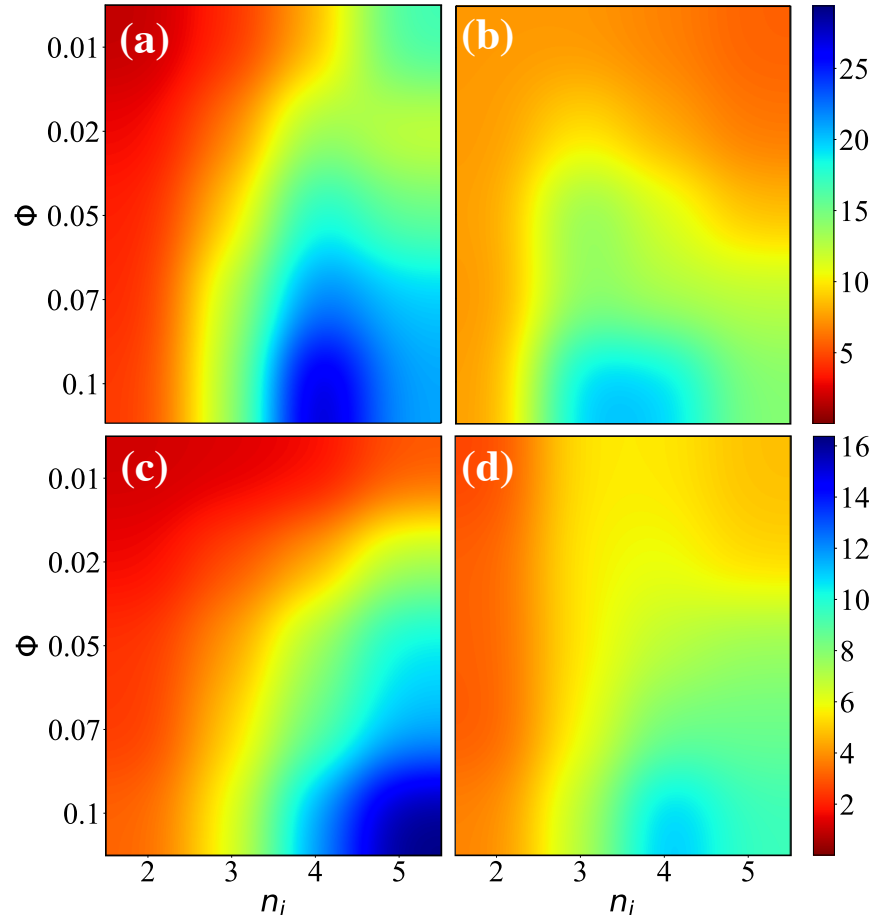


Figure 3: Mean nanoparticles aggregation number for $q = 5, \lambda = 3$ (a), $q = 5, \lambda = 5$ (b), $q = 10, \lambda = 3$ (c) and $q = 10, \lambda = 5$ (d). Each map is obtained as a spline interpolation of the 20 analysed cases.

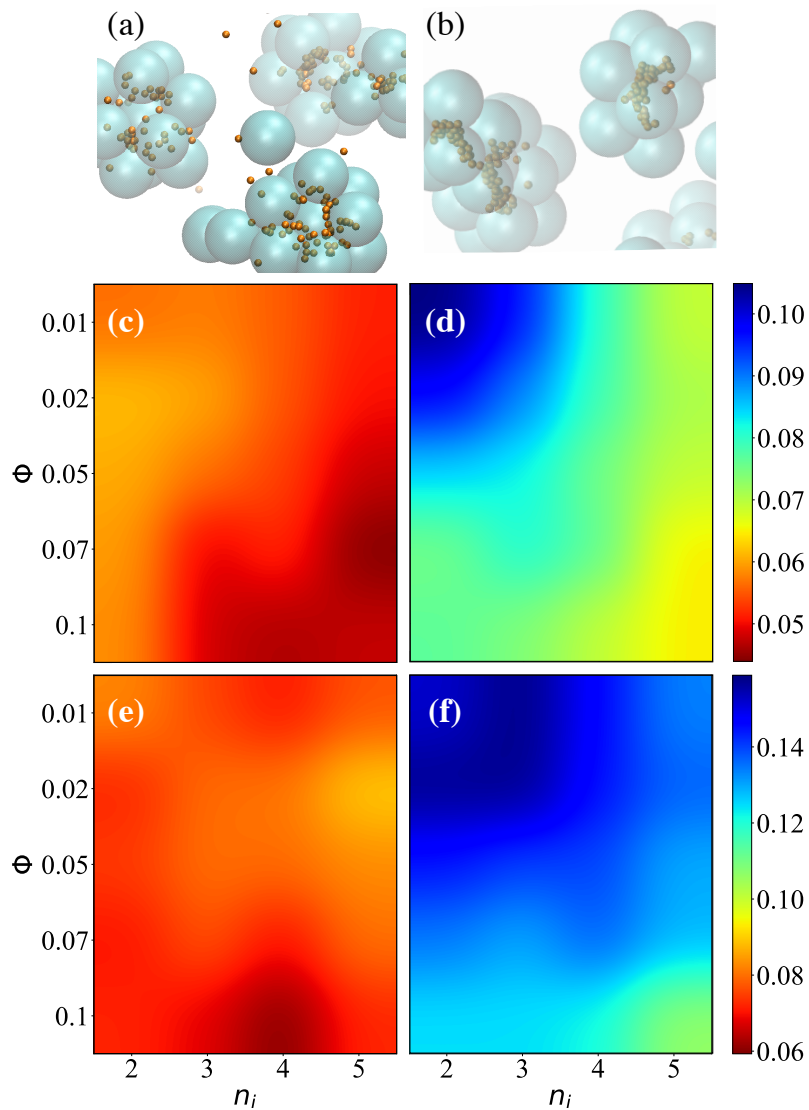


Figure 4: Two typical conformations of clusters presenting ions on the outside - panel (a) - and clusters that are able to adsorb completely ions and insulate them from the solution - panel (b). The measure of the segregation parameter s for $q = 5, \lambda = 3$ (c), $q = 5, \lambda = 5$ (d), $q = 10, \lambda = 3$ (e), and $q = 10, \lambda = 5$ (f). The values of n_i along the horizontal axis are indicated as a multiple of the number of nanoparticles. Each map is obtained as a spline interpolation of the 20 analysed cases.

Discussion

It is interesting to highlight that systems in which the separation between ions and colloids in the aggregates is weakly defined, are those presenting a longer (more MC steps) equilibration time. Such nanocomposites remain for a long time trapped in metastable configurations characterised by elongated stripes - as shown in Figure 5 where the equilibrating region of the energy of a system is shown with its jumps and for each jump a typical conformation of the aggregate is presented.

By comparing computational and experimental results, we can make a few hypotheses on what are the key parameters influencing the two different aggregation paths seen in Figure 1. The hydrated radii of the two ions only differ for about 20%. Such a distinction does not seem enough to justify the different clustering paths observed experimentally for the two binary mixtures, because the computer simulations suggest also that doubling the size ratio from $q = 5$ up to $q = 10$ does not reproduce such a difference in the aggregation scenario.

On the other hand, a slight change in λ drives the self assembly onto two quite different paths: one leading to the formation of aggregates where ions and nanoparticles are quite evenly dispersed within the clusters, and another that shows a strong separation between ions and nanoparticles. Since Co^{2+} and Ni^{2+} ions are at closely related positions in the transition metal series, they lead to a similar behaviour of the two ions in aqueous solution.³¹ Both Ni and Co exist as divalent hexahydrated ions in dilute aqueous solution, but the different electronic structure renders the rate of water exchange on Ni^{2+} lower than that of Co^{2+} .³² This likely seems to lead to the different capability of the two ions to interact with the AgNPs in aqueous solution because the ions are coordinated to AgNPs by the cross-interaction mediated by the water molecules. The different water exchange rate appears to be responsible for the induction of a stronger effective interaction between AgNPs and Ni^{2+} .

It is experimentally shown, Figure 2, that upon augmenting density of ions in solution, the mixtures of AgNPs and Ni^{2+} form bigger and more polydisperse clusters with respect to mixtures of AgNPs and Co^{2+} . The computational analysis performed in this work highlights

that the main parameter leading to different assembly behaviours in the binary mixtures is the effective interaction between the two colloidal species analysed. In fact doubling the radius of the smaller nanoparticles ($q = 5$) induces the assembly of slightly bigger clusters with respect to $q = 10$ (panels (a) and (c) of Figure 3), while a 60% change in the effective interaction has much more evident effect on the clustering process (panels (b) and (d) of Figure 3). The case of stronger effective interaction also leads to more defined clusters quantified by a bigger segregation parameter s (panels (d) and (f) of Figure 4) while a difference in size ratio has a very weak effect on the way ions are adsorbed within the aggregates (panels (c) and (e) of Figure 4). More defined clusters tend not to grow much when the number of ions in solution is increased (panels (b) and (d) of Figure 3), similarly to what happens to the case of clusters formed by the mixture AgNPs and Co^{2+} whose mean aggregation number is seen to grow less dramatically than the ones formed by AgNPs and Ni^{2+} (see left panel of Figure 2). Less defined clusters (panels (a) and (c) of Figure 3) experience a strong effect in the mean aggregation number when the amount of ions in solution is increased, similarly to what happens to the experimentally quantified mixtures of AgNPs and Ni^{2+} (left panel of Figure 2).

Conclusions

In conclusion, in aqueous solution, AgNPs/ Co^{2+} and AgNPs/ Ni^{2+} binary mixture have been shown to self-assemble into aggregates that - experimentally - are either almost packed or branched. Exploiting MC simulations, this work relates the hydration of the ions to an effective interaction potential between ions and nanoparticles. By analysing separately the effect of the effective size ratio due to the hydration process, and a stronger or weaker interaction potential between the two components, the simulations show that internal structure of the aggregates is dominated by the crossed ion/nanoparticle interaction. While a large difference in the size ratio between ions and nanoparticles does not strongly influence the internal

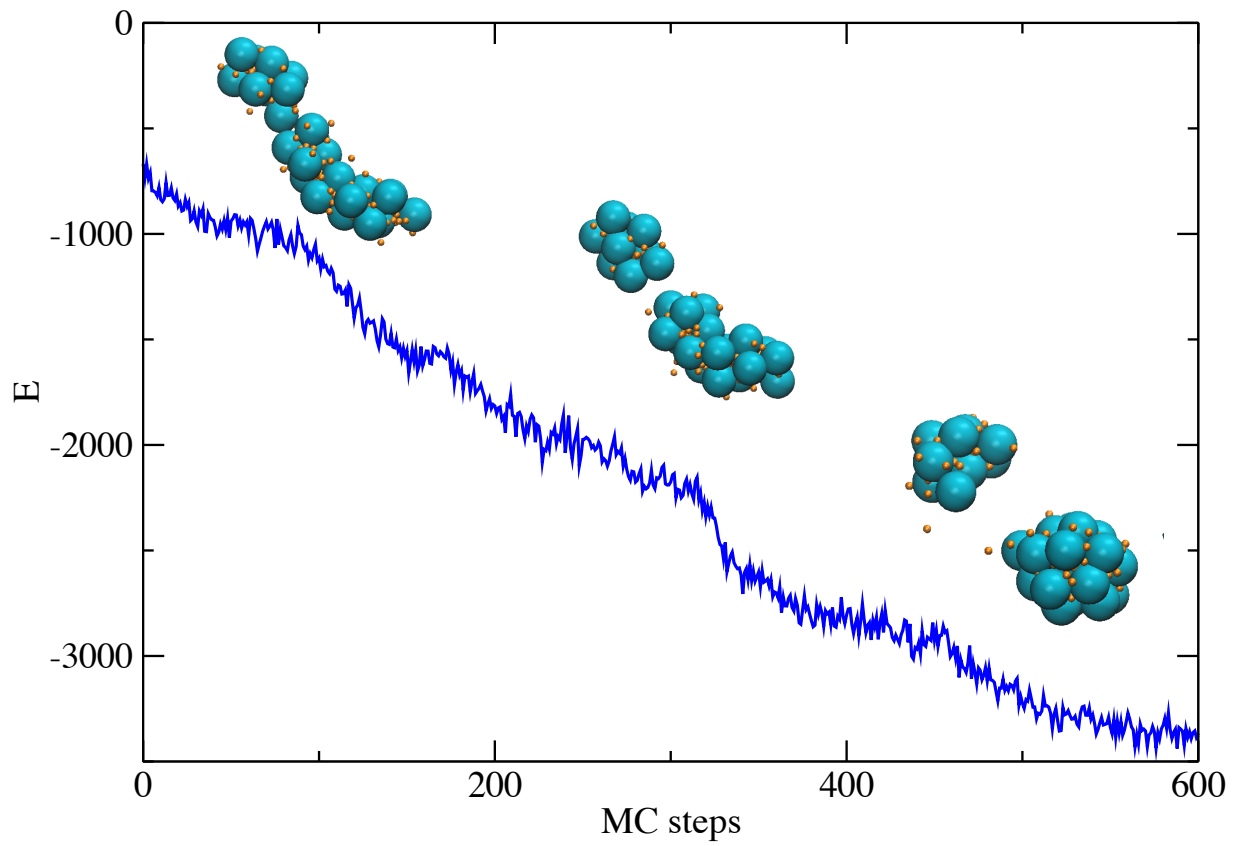


Figure 5: Subset of the equilibration energy showing the change in shape of the aggregates corresponding to equilibration jumps. Each MC step is made of 10^6 MC moves

structure of the aggregates, a change in the crossed interaction drives the self-assembly process onto two completely different paths. Branched clusters are formed by binary mixtures where the crossed interactions are weak, so that ions remain on the surface of the clusters and do not get completely adsorbed by the nanoparticles. As a result these systems remain trapped in metastable states made of elongated clusters that, at equilibrium, will reach a micellar like structure. Conversely a stronger interaction between ions and nanoparticles favours the segregation of the two components, hence rendering the nanoparticle a optimal ion adsorbers. As a concluding remark, functionalised AgNPs appear to be a quite promising way to perform a two-step filtration of metallic ions in solution: the tunability of the adsorption process by means of the two parameters (q, λ) allows to design and realise particles able to cluster into aggregates of predictable size, that at the same time are able to completely adsorb and insulate ions from the solution. While q can be easily tuned via the NP size, the λ parameter can be as well controlled by the grafting density of thiols onto the AgNPs. We presented a simple and effective theoretical model supported by experimental data, explaining and predicting the main AgNPs parameters that determine selective adsorption of Ni^{2+} and Co^{2+} ions in water.

Acknowledgments

The authors thank Prof. M.A. Ricci, Dr E. Bianchi and Dr. T. Gasperi for useful discussions. The authors would like to thank Dr. S. Casciardi for the TEM characterizations. BC acknowledges funding from the Marie Curie Individual Fellowship, project ID 751255. The Grant of Excellence Departments, MIUR-Italy (ARTICOLO 1, COMMI 314 - 337 LEGGE 232/2016) is gratefully acknowledged.

Conflict of interest disclosure

The authors declare no conflict of interest.

Author Contributions

B.C. designed the research, P.C. performed the simulations, I.V., C. B., C.M., P.P., F.B and F. M. performed the experiments. All the authors wrote the manuscript and discussed the research.

Additional informations

Available free of charge via the Internet at <http://pubs.acs.org>.

References

- (1) Rajaganapathy, V.; Xavier, F.; Sreekumar, D.; Mandal, P. Heavy Metal Contamination in Soil, Water and Fodder and their Presence in Livestock and Products : A Review. *Journal of Environmental Science and Technology* **2011**, *4*, 234–249.
- (2) Jarup, L. Impact of environmental pollution on health: balancing risk. *Br. Med. Bull.* **2003**, *68*, 167–182.
- (3) Pedrero, M.; Campuzano, S.; Pingarron, J. M. Quantum Dots as Components of Electrochemical Sensing Platforms for the Detection of Environmental and Food Pollutants: a Review. *J. AOAC Int.* **2017**, *100*, 950–961.
- (4) Zhiyang, Z.; Han, W.; Zhaopeng, C.; Xiaoyan, W.; Jaebum, C.; Chen, L. Plasmonic colorimetric sensors based on etching and growth of noble metal nanoparticles: Strategies and applications. *Biosensors & Bioelectronics* **2018**, *114*, 52–65.
- (5) Li, M.; Gou, H.; Al-Ogaidi, I.; Wu, N. Nanostructured Sensors for Detection of Heavy Metals: A Review. *ACS Sustainable Chemistry & Engineering* **2013**, *1*, 713–723.

- (6) Bhattacharjee, Y.; Chatterjee, D.; Chakraborty, A. Mercaptobenzoheterocyclic compounds functionalized silver nanoparticle, an ultrasensitive colorimetric probe for Hg(II) detection in water with picomolar precision: A correlation between sensitivity and binding affinity. *Sens. Actuators B Chem.* **2018**, *255*, 210–216.
- (7) Ciotta, E.; Paoloni, S.; Richetta, M.; Proposito, P.; Tagliatesta, P.; Lorecchio, C.; Venditti, I.; Fratoddi, I.; Casciardi, S.; Pizzoferrato, Sensitivity to Heavy-Metal Ions of Unfolded Fullerene Quantum Dots. *Sensors* **2017**, *17*, 2614.
- (8) Priyadarshini, E.; Pradhan, Gold nanoparticles as efficient sensors in colorimetric detection of toxic metal ions: A review. *Sens. Actuators B Chem.* **2017**, *238*, 888–902.
- (9) Dinh, V.-P.; Le, N.-C.; Tuyen, L. A.; Hung, N. Q.; Nguyen, V.-D.; Nguyen, N.-T. Insight into adsorption mechanism of lead(II) from aqueous solution by chitosan loaded MnO₂ nanoparticles. *Materials Chemistry and Physics* **2018**, *207*, 294 – 302.
- (10) Lou, T.; Chen, Z.; Wang, Y.; Chen, L. Blue-to-Red Colorimetric Sensing Strategy for Hg²⁺ and Ag⁺ via Redox-Regulated Surface Chemistry of Gold Nanoparticles. *ACS Applied Materials & Interfaces* **2011**, *3*, 1568–1573, PMID: 21469714.
- (11) Fu, X.; Lou, T.; Chen, Z.; Lin, M.; Feng, W.; Chen, L. “Turn-on” Fluorescence Detection of Lead Ions Based on Accelerated Leaching of Gold Nanoparticles on the Surface of Graphene. *ACS Applied Materials & Interfaces* **2012**, *4*, 1080–1086, PMID: 22264012.
- (12) Simsek, E. B.; Duranoglu, D.; Beker, U. Heavy Metal Adsorption by Magnetic Hybrid-Sorbent: An Experimental and Theoretical Approach. *Separation Science and Technology* **2012**, *47*, 1334–1340.
- (13) Ding, Y.; Wang, S.; Li, J.; Chen, L. Nanomaterial-based optical sensors for mercury ions. *TrAC Trends in Analytical Chemistry* **2016**, *82*, 175 – 190.

- (14) Ramezanzadeh, M.; Asghari, M.; Ramezanzadeh, B.; Bahlakeh, G. Fabrication of an efficient system for Zn ions removal from industrial wastewater based on graphene oxide nanosheets decorated with highly crystalline polyaniline nanofibers (GO-PANI): Experimental and ab initio quantum mechanics approaches. *Chemical Engineering Journal* **2018**, *337*, 385 – 397.
- (15) Chen, L.; Fu, X.; Lu, W.; Chen, L. Highly Sensitive and Selective Colorimetric Sensing of Hg²⁺ Based on the Morphology Transition of Silver Nanoprisms. *ACS Applied Materials & Interfaces* **2013**, *5*, 284–290, PMID: 23237272.
- (16) Ratnarathorn, N.; Chailapakul, O.; Dungchai, W. Highly sensitive colorimetric detection of lead using maleic acid functionalized gold nanoparticles. *Talanta* **2015**, *132*, 613 – 618.
- (17) Zhang, Z.; Chen, Z.; Pan, D.; Chen, L. Fenton-like Reaction-Mediated Etching of Gold Nanorods for Visual Detection of Co²⁺. *Langmuir* **2015**, *31*, 643–650, PMID: 25486441.
- (18) Zhang, Z.; Zhang, J.; Lou, T.; Pan, D.; Chen, L.; Qu, C.; Chen, Z. Label-free colorimetric sensing of cobalt(ii) based on inducing aggregation of thiosulfate stabilized gold nanoparticles in the presence of ethylenediamine. *Analyst* **2012**, *137*, 400–405.
- (19) Sung, H. K.; Oh, S. Y.; Park, C.; Kim, Y. Colorimetric Detection of Co²⁺ Ion Using Silver Nanoparticles with Spherical, Plate, and Rod Shapes. *Langmuir* **2013**, *29*, 8978–8982.
- (20) Sarkar, P. K.; Polley, N.; Chakrabarti, S.; Lemmens, P.; Pal, S. K. Nanosurface Energy Transfer Based Highly Selective and Ultrasensitive “Turn on” Fluorescence Mercury Sensor. *ACS Sensors* **2016**, *1*, 789–797.
- (21) Feng, J.; Jin, W.; Huang, P.; Wu, F. Highly selective colorimetric detection of Ni²⁺ using silver nanoparticles cofunctionalized with adenosine monophosphate and sodium dodecyl sulfonate. *J. Nanopart. Res.* **2017**, *19*, 306.

- (22) Mochi, F.; Burratti, L.; Fratoddi, I.; Venditti, I.; Battocchio, C.; Carlini, L.; Iucci, G.; Casalboni, M.; De Matteis, F.; Casciardi, S.; Nappini, S.; Pis, I.; Proposito, P. Plasmonic Sensor Based on Interaction between Silver Nanoparticles and Ni²⁺ or Co²⁺ in Water. *Nanomaterials* **2018**, *8*, 488.
- (23) Proposito, P.; Mochi, F.; Ciotta, E.; Casalboni, M.; De Matteis, F.; Venditti, I.; Fontana, L.; Testa, G.; Fratoddi, I. Hydrophilic silver nanoparticles with tunable optical properties: application for the detection of heavy metals in water. *Beilstein J. Nanotechnol.* **2016**, *7*, 1654.
- (24) Shannon, R. D. Revised effective ionic radii and systematic studies of interatomic distances in halides and chalcogenides. *Acta Cryst.* **1976**, *A32*, 751.
- (25) Marcus, Y. Thermodynamics of solvation of ions. Part 5. Gibbs free energy of hydration at 298.15 K. *J. Chem. Soc., Faraday Trans.* **1991**, *87*, 2995–2999.
- (26) Huissmann, S.; Blaak, R.; Likos, C. N. Star Polymers in Solvents of Varying Quality. *Macromolecules* **2009**, *42*, 2806–2816.
- (27) Tang, J.; Wu, P.; Hou, X.; Xu, K. Modification-free and N-acetyl-L-cysteine-induced colorimetric response of AuNPs: A mechanistic study and sensitive Hg²⁺ detection. *Talanta* **2016**, *159*, 87–92.
- (28) Suslov, A.; Lama, P.; Dorsinville, R. Fluorescence enhancement of Rhodamine B by monodispersed silver nanoparticles. *Optics Communications* **2015**, *345*, 116–119.
- (29) Oliveira, E.; Nez, C.; Santos, H.; Fernandez-Lodeiro, J.; Fernandez-Lodeiro, A.; Capelo, J.; Lodeiro, C. Revisiting the use of gold and silver functionalised nanoparticles as colorimetric and fluorometric chemosensors for metal ions. *Sensors and Actuators, B: Chemical* **2015**, *212*, 297–328.

- (30) Fratoddi, I. et al. Gold nanoparticles functionalized by rhodamine B isothiocyanate: A new tool to control plasmonic effects. *J. Colloid Interface. Sci.* **2018**, *513*, 10–19.
- (31) Persson, I. Hydrated metal ions in aqueous solution: How regular are their structures? *Pure Appl. Chem.* **2010**, *82*, 1901.
- (32) Flett, D. S. Cobalt-Nickel Separation in Hydrometallurgy: a Review. *Chemistry for Sustainable Development* **2004**, *12*, 81.